# A HIGH-RESOLUTION VIEW OF THE SOLAR CHROMOSPHERE AND CORONA

G.E. Brueckner
E.O. Hulburt Center for Space Research, Naval Research
Laboratory, Washington, D.C.   20375   USA

## INTRODUCTION

Skylab has demonstrated the dominant role of magnetic fields in the solar atmosphere.  The solar wind is not a necessary consequence of the pressure imbalance between the hot corona and the interplanetary medium.  High speed solar windstreams are originating in coronal holes where coronal density and temperature are less than in the quiet sun.  Older models of the solar wind invoke heat conduction from the hot corona as the prime energy source for the solar wind.  However in coronal holes the energy supplied by heat conduction is less than in the ordinary sun while the high speed windstreams require an amount of energy which cannot be supplied by conduction alone.

Other non-thermal energy sources must be found.  Low resolution observations from Skylab and OSO-8 did not uncover any such sources. Because we rely on spectroscopic Doppler measurements to uncover mechanical energy in the solar atmosphere, poor spatial resolution is the reason why progress is slow.  The flux of mechanical energy is proportional to the third power of measured velocities where mechanical energy input results in motions of the gas.  Therefore, a small volume carrying large amounts of energy when superimposed on strong background radiation will have an insignificant impact on the total spatially integrated line profile or Doppler shift.  Other heating mechanisms, like Joule heating, must be tested by intensity measure-ments.  Again, very high spatial resolution is required to separate small fluctuations from the background radiation.  Observations of the chromosphere have been carried out mainly in optically thick lines, where the scattering length of photons is longer than the anticipated dimensions of the fine structures.

The rocket flights of NRL's High Resolution Telescope and Spectrograph instrument, which operates at ultraviolet wavelength (1175-1710 Å simultaneous coverage) with a spectral resolution of 0.06 Å, a spatial resolution of 1 arc sec and a spatial coverage of 0.5 x 1000 arc sec$^2$ have confirmed this picture.  Supersonic

557

motions have been found in the transition zone confined to small
elements.  In addition the time series of spectra show that explosive
events exist which have a rise time of less than 20 seconds.  The
discovery of such fast events has far reaching consequences on the
formation of spectral lines because ionization equilibrium cannot be
assumed anymore.  Furthermore, flows which carry kinetic energy far
exceeding the thermal energy of the plasma exist everywhere on the
solar surface, particularly in the transition zone, making the as-
sumption of hydrostatic equilibrium invalid.

The use of an ultraviolet broadband spectroheliograph has shown
the existence of supersonic motions in the corona as intensity spikes.
Photographed in the transition zone line of C IV they may be identical
with the coronal spikes observed by Koutchmy and Stellmacher (1976).
They have been observed in a coronal hole and because of their high
apparent velocities up to 500 km s$^{-1}$ they may carry enough energy for
the high speed solar windstreams.  They are accelerated at 15,000 km
above the solar surface.  The possibility arises that the solar wind
originates very close to the solar surface and must be considered
a momentum driven wind as proposed by Ivanchuk (1969).  However,
there are indications that the spikes may be parts of high loops
in a coronal hole.  This would support Joule or Alfvén wave heating
theories (Hollweg 1978).

FINE STRUCTURE AND EVOLUTION OF THE TEMPERATURE MINIMUM LAYER

A high resolution photograph of the UV continuum at 1600 Å (band-
pass 40 Å) is shown in Fig. 1.  This spectral region is dominated by
continuum emission thought to originate at the temperature minimum,
although some contribution (<10%) from low chromospheric lines is
included.  Two components can be seen.  Most of the emission originates
from small grains which have a size of 1500 km, close to the resolution
of the instrument.  In addition a hazy component exists in the network
and plages.  The lifetime of the grains vary from 60 seconds to
longer than 240 seconds which is a lower limit given by the duration
of the rocket flight.  Their brightness temperature covers a range
from 4300 K to 4800 K in the quiet sun and 4300 K to 5000 K in plage
regions.  The grains in the plages have lifetimes exceeding the
duration of the rocket flight.  Ten percent of the solar surface are
covered with grains.  The image shows that the magnetic structure of
the sun is already strongly visible at the temperature minimum.  A
close inspection of the images indicate that each individual grain
seems to be a part of a small loop, although higher resolution obser-
vations are required to confirm this.  The possibility cannot be
excluded that a magnetic heating mechanism is working at layers as
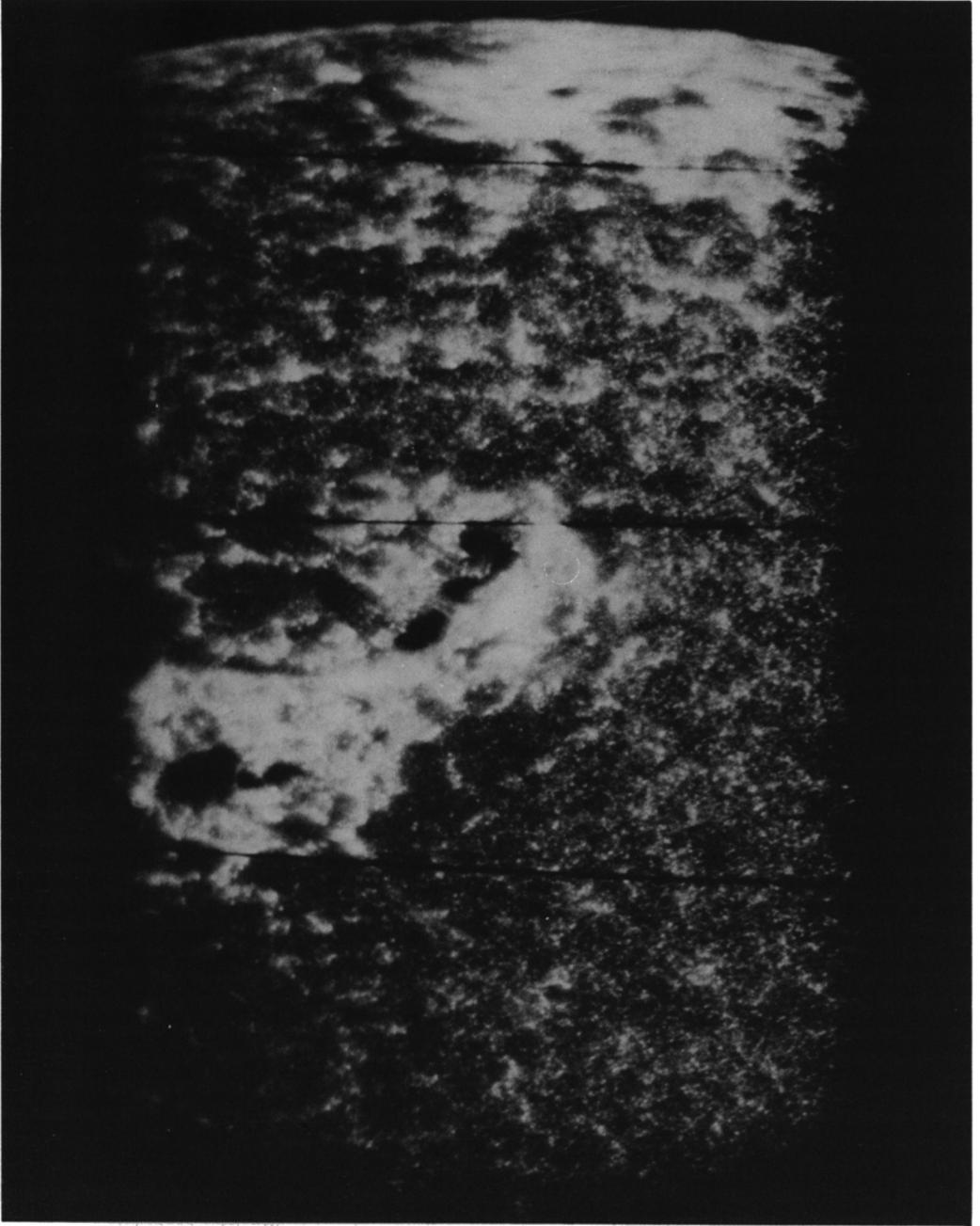deep as the temperature minimum.

Fig. 1: High resolution image of the 1600 Å solar continuum, bandpass 40 Å. The solar limb is at the top, solar center at the bottom.

FINE STRUCTURE AND DYNAMICS OF THE TRANSITION ZONE

Transition zone line emission of the quiet sun is confined to
areas of dark mottles in Hα off band images.  Our photometry with
improved spatial resolution shows that the intensity of the C IV
lines outside the dark mottles is as low or lower than 1/20 of the
intensity in dark mottle areas.  Therefore, most of the transition
zone line emission originates in dark mottle areas, which are the
location of spicules.

Line profiles of high spatial resolution C IV spectrograms as
shown in Fig. 2 can be separated into 3 categories:

(1) Thermal or near thermal profiles in filaments or centers of
    supergranulation cells areas.

(2) Multicomponent broad profiles in correlation with dark
    mottles.

(3) Non-thermal broad line profiles of explosive events.

This categorization has been made based on the following different
properties of the profiles.

Thermal or near thermal profiles have small changes in line
width and Doppler shifts with time, although they are not static.
Their width is close to the thermal width.

The majority of the emission is found in the multicomponent
profiles.  A strong background component is always visible at the
rest wavelength.  Doppler shifted components are added to the red and
blue wing.  The intensity of the red wing components by far exceeds
that of the blue wing.  Time changes of the red wing components are
slower than those in the blue wing.  The profiles can be synthesized
by Doppler-shifted thermal components.  One has the impression that
each profile represents the overlapping emission from still spatially
unresolved elements moving with different Doppler velocities.  However,
we cannot exclude the possibility that the red-asymmetric profiles are
caused by a particular form of turbulence in the transition zone.

A tachogram of one spectrum is shown in Fig. 3.  The line
asymmetries at half and quarter peak intensity have been measured in
the framework of low chromospheric Si I lines, which show much smaller
shifts than the C IV lines.  However, the rest position of the C IV
lines depends on any possible systematic shift of the Si I lines
which are assumed to be at their rest wavelength.  We estimate that
our systematic error of the zero velocity is $\pm 3$ km s$^{-1}$.  At the left
the slit covered a filament where no systematic velocities are
observed.  In the following plage two distinct areas are visible,
one with strong red shifts and another one with material at rest.
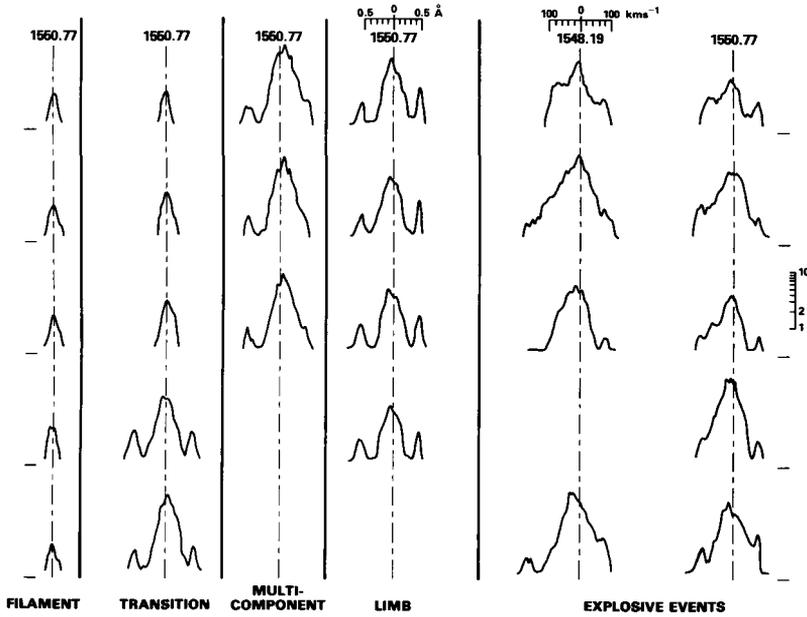The following quiet sun areas show very strongly fluctuating line

Fig. 2:   Typical C IV line profiles, 1 arc second spatial resolution.
One notes the rapid change of the profiles in a region
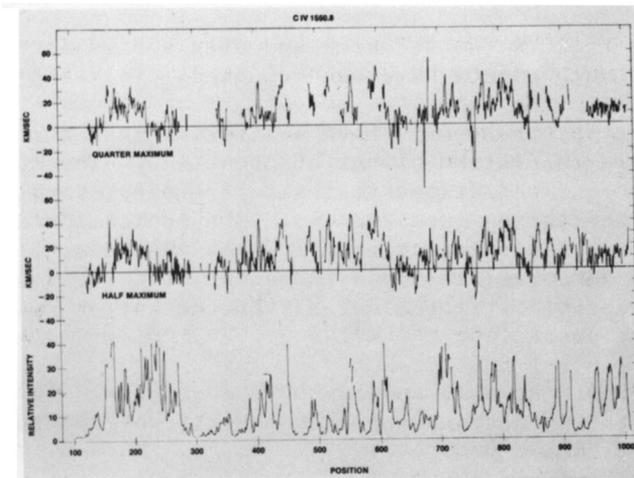between cell interior and boundary (marked "transition").



Fig. 3:   Tachogram of C IV 1550 A.  Bottom:  relative intensities,
Center:  line asymmetry at half maximum intensity, Top:
line asymmetry at quarter maximum intensity.  Positive
values are red shifts, negative values blue shifts.  Solar
center is at position 100, limb at position 1000.

asymmetries from point to point. The largest velocities observed are 30 km sec$^{-1}$ to the red. They occur usually in patches of 5-8 arc sec and are concentrated in the dark mottle areas. The strong dominance of red asymmetries is obvious. The limb profiles are at the rest wavelength. This is a result of averaging over a long line of sight.

Particle flux and kinetic energy flux in the downward moving material has been estimated to be between $1.6 \times 10^{15}$ and $1.6 \times 10^{16}$ cm$^{-2}$ sec$^{-1}$ and $2 \times 10^4$ to $2 \times 10^5$ ergs cm$^{-2}$ sec$^{-1}$, respectively, averaged over the whole sun. Mass and energy flux in the downward component can only be compensated by equivalent flows in the explosive events if these carry a larger amount of material than that expected from ionization equilibrium. Because of the very short rise time of the explosive events they are in a state of transient ionization. They may be caused by shockwaves or electromagnetic forces which heat chromospheric material very rapidly to higher temperatures, with subsequent ejection into the corona. The downward flowing component then represents the cooling and recombining gas.

The profiles of explosive events are distinctly different. They are confined to small areas and have non-Gaussian shapes. Shifted components can be seen as far out at 70 km s$^{-1}$ into the blue and red wing. They are confined to small areas and have non-Gaussian shapes. The blue wings are usually stronger than the red wings.

The spatial resolution of the instrument is crucial to make these profiles visible against the strong background emission.

In an area of 10 x 800 arc sec$^2$ and over a time interval of 260 sec, 145 of such events have been counted.

The majority of the events have a lifetime less than 20 sec which is the time resolution of our observations. The long lived events show strong fluctuations in their intensity, sometimes disappearing and reappearing (see Fig. 4). The ionization and recombination time of C IV is longer than 10 sec. Therefore, we may see here transition zone material in a transient state of ionization and consequently underestimate considerably the amount of material involved in the explosive events.

A time sequence of C IV spectra of the quiet sun is shown in Fig. 4. We cannot detect any periodic behavior of Doppler shifts or intensity fluctuations.

Figure 5 shows a C IV time series of the largest explosive event observed so far in an otherwise inconspicuous area of the quiet sun. Plasma is accelerated several times to velocities up to 400 km s$^{-1}$ before it leaves the spectrograph slit. The last event can be interpreted as an exploding loop. The observed velocities are supersonic in the corona and must cause strong shock waves.
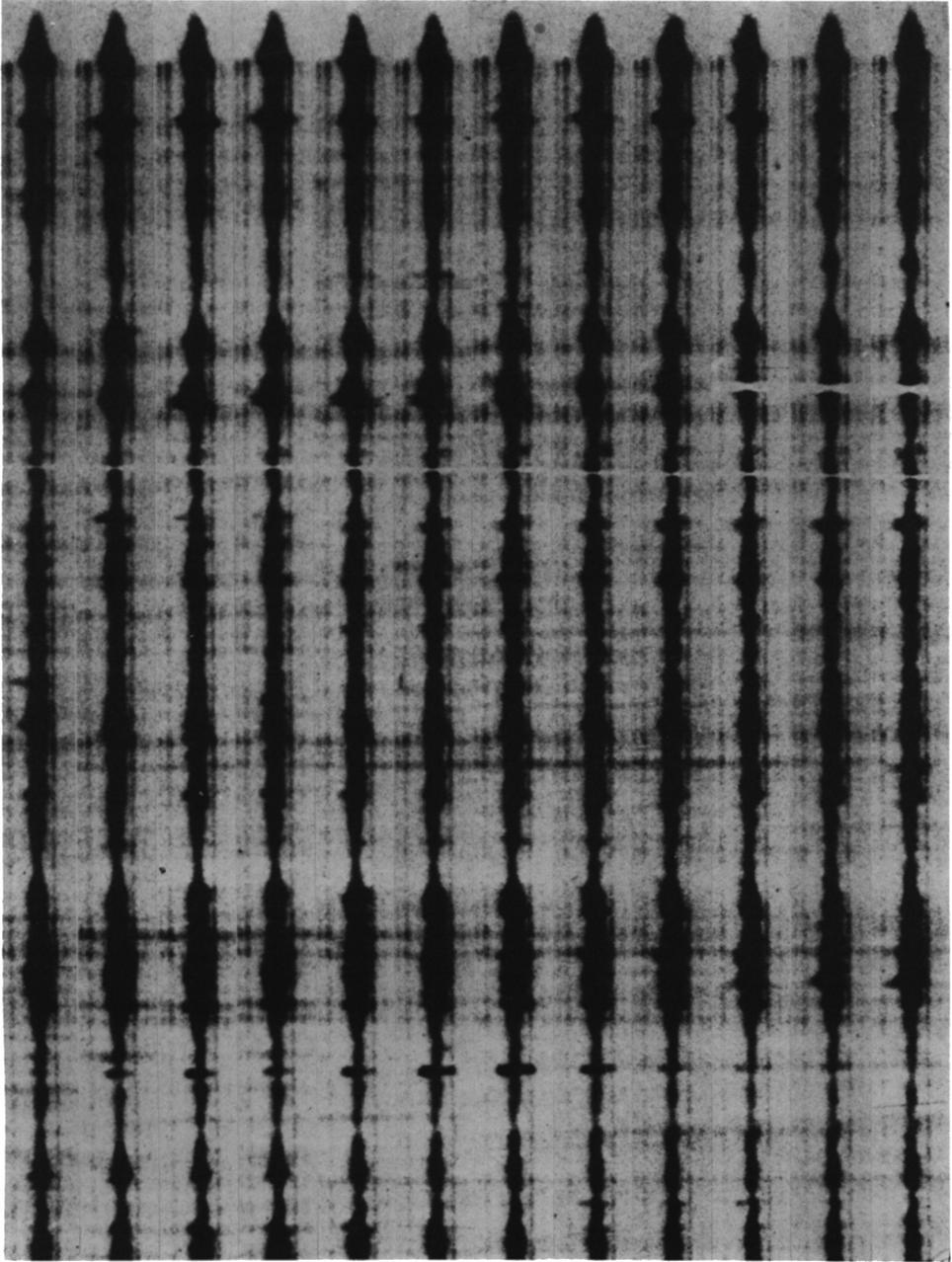
Fig. 4: Time sequence of C IV spectra taken in 20 second intervals. Solar limb is at the top, the spectra cover 1/2 of a solar radius.
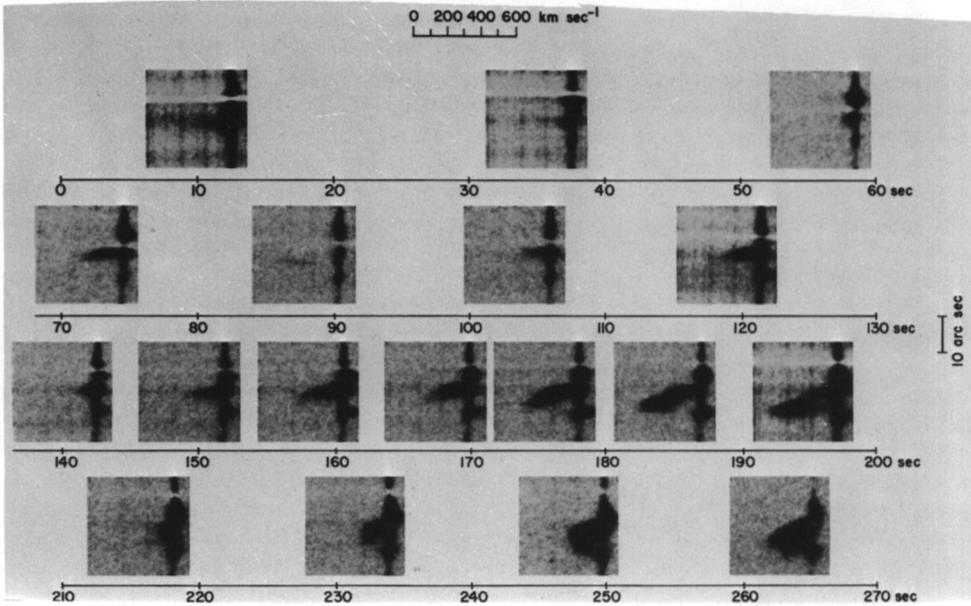
Fig. 5:   Large explosive events recurring at same location. Exploding
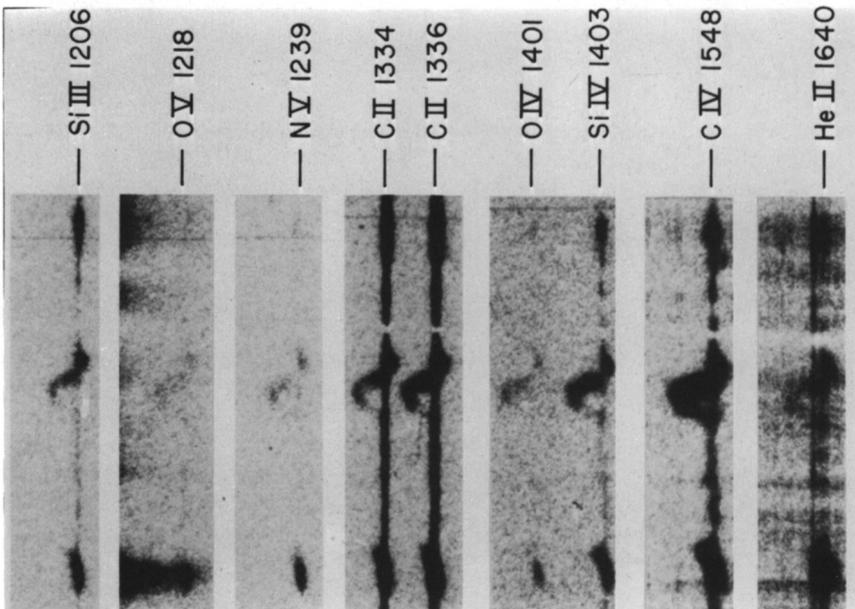          loop 210-260 sec.



Fig. 6:   The exploding loop shown in several spectral lines. Comparing
          the Doppler-shifted intensities (center) with the "quiet" sun
          (bottom and top), one sees that the exploding event has a
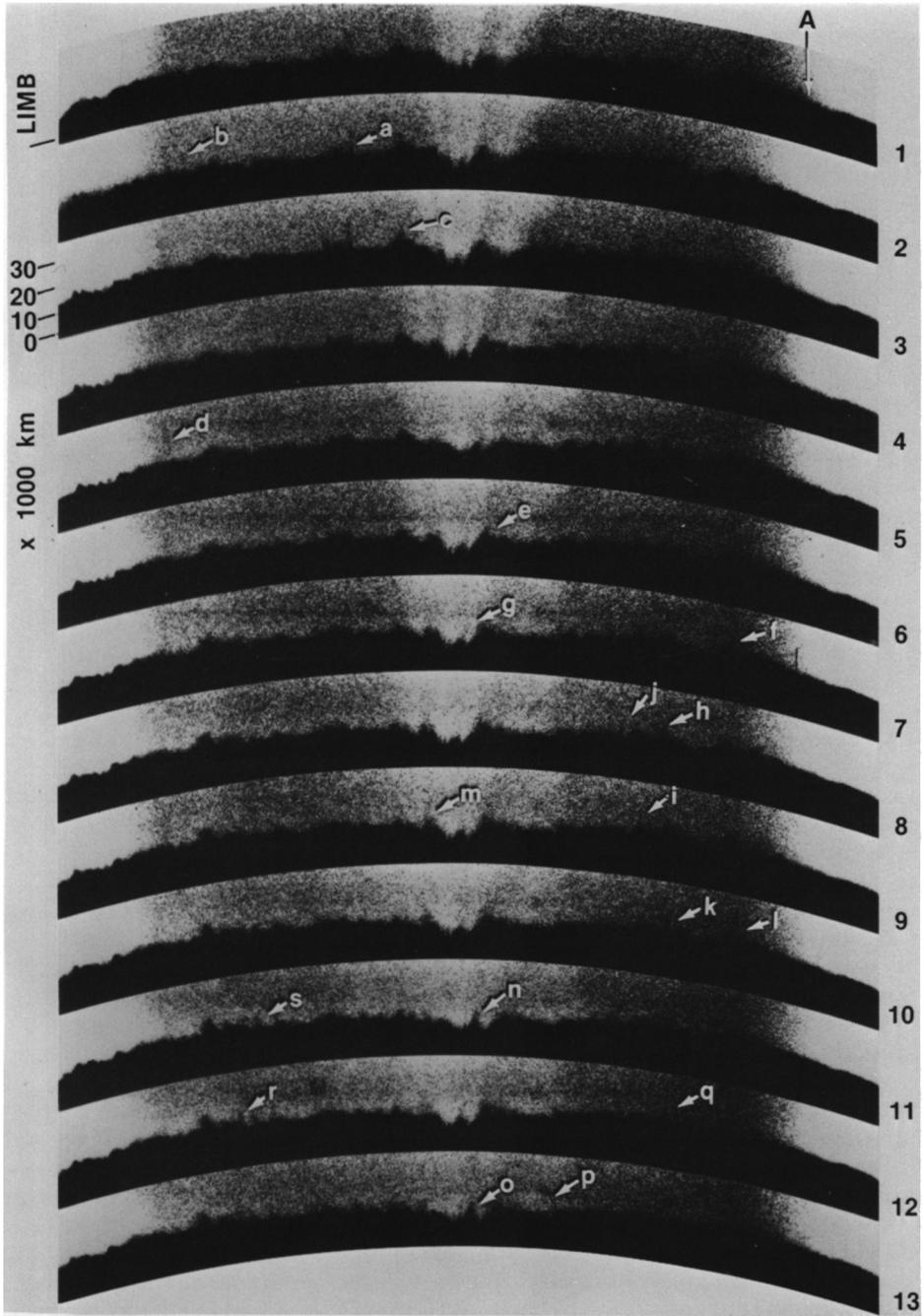          maximum emission measure as ~100,000 K.

Fig. 7:  Time sequence of C IV spectroheliograms of a polar cap.
         Time interval 20 sec.

As can be seen in Fig. 6, the emission measure vrs. temperature distribution of the explosive event is opposite to that observed in the average sun. The explosive events show a <u>maximum</u> emission measure at 100,000 K, while the average sun has a <u>minimum</u> emission measure at this temperature.

The appearance of all these processes in the spicule producing areas makes one suspect that spicules and the dynamics of the transition zone are both manifestations of the same physical process.

## C IV SPECTROHELIOGRAMS OF A CORONAL HOLE

Fig. 7 shows a series of 3/4 sec exposures taken at 20 second intervals with a broadband ($\lambda = 1550 \pm 100$ Å) spectroheliograph at a polar cap. The overexposed images of the disk contain mostly continuum emission and in addition all emission lines in the 200 Å wide wavelength band. Above the limb however at 10,000 km altitude the continuum and chromospheric lines should have disappeared and the images are primarily C IV emission. The visible structures fall into two categories: (a) large structures from 2 to 10 arc sec in size which have heights of 10,000 to 17,000 km above the white light solar limb. If one follows a single event one notes that after reaching its peak altitude it loses altitude faster than one would expect from gravitational forces. This means that it either is squeezed down by magnetic forces or that the observed motions are not material flows. They may be the transient of an excitation mechanism. It is very likely that these structures are identical with the macro-spicules observed in He II (Bohlin et al. 1975) and they are responsible for the "thicker" transition zone in polar caps. (b) Distinctly different structures are the spikes which are marked with small case letters in Fig. 7. They expand outwardly with velocities from 240 to 800 km s$^{-1}$, and disappear within less than 20 to 40 seconds. Their diameter seems to be the resolution limit of the instrument (~2 arc sec). They extend from the top of the macrospicules (10,000 - 17,000 km) up to 25,000 km. Twenty-three events can be seen in the sequence, which lasted 240 seconds. The spikes seem to originate from the top of macrospicules. In some cases one has the impression, that they are short lived loops, however the resolution of these observations is insufficient to draw a final conclusion. Koutchmy and Stellmacher (1976) analyzed a coronal "spike". They found a diameter of 1 arc sec and an electron density of $N_e \approx 1 \times 10^{10}$. They assumed that the spike is at coronal temperatures because of its color index so that they could exclude chromospheric emission. Our C IV observations may trace the same kind of spike. It is entirely plausible to assume that these spikes are a multithermal plasma. There may be genuine material move-ment on the transient of an excitation front like an Alfvén wave or an electric current. The largest explosive event observed spectroscopically in the quiet sun (see Fig. 5 and 6) showed material velocities up to 400 km s$^{-1}$. However, such events are very rare in the quiet sun which does not exclude that they are more common in coronal holes.

Either explanation - excitation front or material movement - requires
the existence of small scale magnetic fields. For $N_e \sim 1 \times 10^{10}$
and $T_e \sim 1 \times 16^6$ a minimum field strength of 6 gauss is required
to prevent expansion of the spike which leads to an Alfvén speed of
130 km s$^{-1}$.

## JOULE HEATING OF THE SOLAR ATMOSPHERE

The stochastic nature of the observations discussed in the
previous sections may be explained by rapid energy dissipation of
new emerging magnetic flux.

Syrovatskii (1976) has pointed out, that dissipation of magnetic
energy in a current sheet leads to instabilities at $8 \times 10^4$K, because
radiation losses cannot compensate the Joule heating of the plasma.
Our observations of the explosive events are in agreement with this
prediction. At $1 \times 10^5$K, where the C IV lines are formed, we observe
a maximum of turbulence. Strong, granular size ($b = 7 \times 10^7$ cm)
magnetic fields of 1500 gauss have been observed in the network.
Therefore, we can assume field gradients of

$$\frac{dB}{dx} = \frac{1500}{7 \times 10^7} = 2 \times 10^{-5} \frac{Gauss}{cm}$$

To estimate the total power output from a neutral sheet we fol-
low Syrovatskii (1976). The total power dissipated by such a current
sheet is just

$$P_T \sim J^2/\sigma \ \Delta V$$

where $\sigma$ is the Coulomb conductivity, $\Delta V$ = abl, a being the thickness
of the sheet, b its width and l its length. The current density J
one estimates using Ampere's equation so that $P_T$ becomes

$$P_T \sim \frac{c^2}{16\pi^2} \frac{B^2}{a\sigma} b\ell$$

where B is the average field strength of the sheet. Taking B $\sim$ 1500 g,
$\sigma \sim 3.2 \times 10^{14}$, b=1$\sim$7x10$^7$ and at $\sim$10 cm we find $P_T \sim 3 \times 10^{25}$ ergs/sec.

At T $\sim 8 \times 10^4$K the plasma is squeezed out of the current sheet
with the Alfvén velocity. From the observations it follows
$V_{AS} \sim 7 \times 10^6$ cm s$^{-1}$. We use Syrovatskii's relations to calculate
the density $n_s$ inside and $n_o$ outside the current sheet as well as
the electron drift velocity $V_d$

$$V_x^2 \equiv V_{AS}^2 = \frac{B_s^2}{4Mn_s\pi} \; ; \quad V_d = \frac{cE_o}{B_s} \; ; \quad n_oV_db = n_sV_xa$$

and obtain

$$n_s = 2.3 \times 10^{15} \text{ cm}^{-3}; \; n_o = 1 \times 10^{11} \text{ cm}^{-3}; \; V_d = 2.2 \times 10^4 \text{ cm sec}^{-1}$$

Basri et al. (1979) and Nicolas et al. (1979) determine $n_o =$ 5 x $10^{10}$ at T ~ 3 x $10^4$K. The instability should start at this temperature, which is characteristic for the upper chromosphere.

The birthrate of the explosive events averaged over the whole sun can be estimated from the observations to be

$$R_{av} \sim 8 \times 10^2 \text{ events sec}^{-1}$$

Their average lifetime t is 20 sec. Therefore the total energy flux averaged over the solar surface dissipated in such currents sheets is

$$F_E = \frac{P_T t R_{av}}{A} \sim 5 \times 10^6 \text{ ergs cm}^{-2} \text{ sec}^{-1}$$

where A is the surface area of the sun. $F_E$ can account for the chromospheric, transition zone and coronal radiation losses.

According to Syrovatskii, the duration of the eruptive phase of a current sheet is given by the relation

$$t_z = \frac{b}{V_{AS}} \sim 10 \text{ sec}$$

which is also in agreement with the observations. Approximately half of the events have a lifetime $t_z < 20$ sec which is the time resolution of our observations, while others can last as long as 200 sec. However, the long lasting events show larger dimensions of up to 7 x $10^8$ cm, which is in agreement with the above relationship given by Syrovatskii.

It can be estimated that the kinetic energy of the plasma turbulence is rather small, therefore most of the energy dissipated in the current sheet is released as Joule heating. Unfortunately our observations cannot answer the question whether this mechanism can produce plasma at coronal temperatures. However, Syrovatskii

points out that a rapid heating to coronal temperatures takes place after the onset of the turbulent phase at $8 \times 10^4$K. Skylab observation (Brueckner et al. 1976) have shown very strong (400 km s$^{-1}$) short time turbulence at low coronal temperatures in an emerging flux region.

In conclusion, the observation of loops in all layers of the solar atmosphere together with realization of very rapid time changes and supersonic motions make it very likely that the heating of the outer solar atmosphere as well as the energy needed for the propulsion of the solar wind, is caused by magneto-acoustic waves or electric currents.

REFERENCES

Basri, G.S., Linsky, J.L., Bartoe, J.-D.F., Brueckner, G.E., VanHoosier, M.E.: 1979, Ap. J. 230, 924.
Bohlin, J.D., Vogel, S.N., Purcell, J.D., Sheeley, N.R., Tousey, R. and VanHoosier, M.E.: 1975, Ap. J. Letters 197, L133.
Brueckner, G.E., Patterson, N.P. and Scherrer, V.E.: 1976, Solar Phys. 47, 127.
Hollweg, J.V.: 1978, Solar Phys. 56, 305.
Ivanchuk, V.I., Vsekhsvjatsky, S.K., Dzubenko, N.I. and Rubo, G.A.: 1969, Astr. Circ. 504, 1.
Koutchmy, S. and Stellmacher, G.: 1976, Solar Phys. 49, 253.
Nicolas, K.R., Bartoe, J.-D.F., Brueckner, G.E., VanHoosier, M.E.: 1979, to appear in Ap. J., Sept. 1.
Somov, B.V. and Syrovatskii, S.I. 1977: preprint #27, P.N. Lebedev Physical Institute, I.E. Tamm Department of Theoretical Physics, Moscow.
Syrovatskii, S.I.: 1976, Sov. Astron. Letters 2, 13.